Supplementary information

Designing Ru-doped $Zn_3V_3O_8$ Bifunctional OER and HER Catalyst Through a Unified Computational and Experimental Approach

Xuyan Zhou[a,d], Xiaowei Tang[c], Haitao Xu[b], Tao Jiang[a], Kailong Hu[a,d], Hua-Jun Qiu[a,d*], and Xi Lin[a,d,e*]*

[a]*School of Materials Science and Engineering, Harbin Institute of Technology, Shenzhen 518055, P. R. China*

E-mail: qiuhuajun@hit.edu.cn,

linxi@hit.edu.cn

[b]*School of Materials Science and Engineering, Dongguan University of Technology, Dongguan 523808, China*

E-mail: xuht@dgut.edu.cn

[c]*Mathematical School, Qilu Normal University, Jinan 250200, China*

[d]*Blockchain Development and Research Institute, Harbin Institute of Technology, Shenzhen 518055, P.R. China*

[e]*State Key Laboratory of Advanced Welding and Joining, Harbin Institute of Technology, Harbin 150001, P. R. China*

Theoretical Section

Spin-polarized density functional theory (DFT) calculations were carried out with the Vienna ab initio Simulation Package (VASP)[1,2] which uses the projector augmented wave (PAW) pseudo-potentials[3]. For the exchange-correlation functional we used the Perdew-Burke-Ernzerhof (PBE)[4] within the generalized gradient approximation (GGA). As spinel ferrites are strongly correlated systems, static electronic correlations were taken into account within the GGA+U method[5], where a U value of 3.25 eV was employed for V[6]. The cutoff energy of 500 eV was adopted. Based on the previous work, $Zn_3V_3O_8$ can be obtained by partially substituting V atoms by Zn atoms in ZnV_2O_4. The crystallographic data of ZnV_2O_4 can be found in crystallography open database (COD, reference no. 9012331). The [001]-oriented surfaces were simulated using slabs with 4 atomic layers and lattice vectors of $\mathbf{a_1} = \mathbf{a} + \mathbf{b}$ and $\mathbf{b_1} = -\mathbf{a} + \mathbf{b}$ (a, b are the primitive vectors) for all simulations. A vacuum thickness of 12 Å was inserted to minimize the artificial interactions among the supercell images. All the atomic structures were fully relaxed until the forces on each atom being less than 0.02 eV/Å and the energy variation between two iterations being less than 1×10^{-5} eV. During the structural relaxation, the bottom layer metal atoms were constrained to mimic the structure of a semi-infinite solid. The Brillouin zone of each slab was sampled by a Monkhorst-Pack k-point mesh of 4 × 4 × 1 for geometry optimization and an 8 × 8 × 1 k-mesh for density of states (DOS) calculations, respectively. The Grimme's semiempirical DFT-D3 scheme of the dispersion correction was adopted to describe the van der Waals (vdW) interactions.

Water splitting is considered as two half reactions: OER and HER. Usually, the overall OER reaction is the four-electron reaction pathway.

$$4OH^- \rightarrow O_2(g) + 2H_2O(l) + 4e^- \quad \text{(S1)}$$

A widely used approach to model OER considers the formation of four reaction intermediates on the surface:

$$OH^- + * \rightarrow *OH + e^- \quad \text{(S2)}$$

$$OH^- + *OH \rightarrow *O + H_2O(l) + e^- \quad \text{(S3)}$$

$$OH^- + *O \rightarrow *OOH + e^- \quad (S4)$$

$$OH^- + *OOH \rightarrow * + O_2(g) + H_2O(l) + e^- \quad (S5)$$

where * represents the catalyst surface and *OOH, *O and *OH species are oxygenated intermediates. The reaction free energy of each step can be calculated by

$$\Delta G = \Delta E_{DFT} + \Delta ZPE - T\Delta S - eU \quad (S6)$$

where ΔE_{DFT}, ΔZPE and ΔS are the energy changes in the DFT total energy, zero-point energy and entropy from the initial state to the final state, respectively. ZPE is obtained from vibrational frequency calculation. As for H_2O and H_2 molecules, their entropy values are taken from the NIST-JANAF thermodynamics table[7]. For each adsorbate, their entropy values are computed based on (ZPE - TS) taken from VASPKIT[8] and ZPE. The theoretical overpotential η is determined by the potential limiting step:

$$\eta = \Delta G_{max}/e - U_0 \quad (S7)$$

In order to establish trends in reactivity, the overpotential is often related to binding energy differences. The binding energy of the intermediate species to the surface are defined as:

$$\Delta G_{*O} = E_{*O} - E_* - E_{H2O} + E_{H2} + \Delta ZPE - T\Delta S \quad (S8)$$

$$\Delta G_{*OH} = E_{*OH} - E_* - E_{H2O} + (1/2)E_{H2} + \Delta ZPE - T\Delta S \quad (S9)$$

$$\Delta G_{*OOH} = E_{*OOH} - E_* - 2E_{H2O} + (3/2)E_{H2} + \Delta ZPE - T\Delta S \quad (S10)$$

where E_*, E_{*O}, E_{*OH} and E_{*OOH} are the DFT total energies of a clean catalyst surface and that absorbed by a O, OH and OOH species, respectively; E_{H2O} and E_{H2} are the energies of a H_2O and H_2 molecule in a vacuum, respectively.

For HER, the overall reaction is

$$H_2O(l) + e^- \rightarrow 1/2H_2(g) + OH^- \quad (S11)$$

A widely used approach to model HER considers the formation of the following reaction intermediate on the surface.

$$H_2O(l) + e^- + * \rightarrow *H + OH^- \quad (S12)$$

The calculated reaction free energy (ΔG_{*H}) under electrode potential U = 0 V can be calculated by:

$$\Delta G_{*H} = E_{*H} - E_{*} - (1/2)E_{H2} + \Delta ZPE - T\Delta S \quad \text{(S13)}$$

The optimal value for HER is $\Delta G_{*H} = 0$, which means that the smaller the $|\Delta G_{*H}|$, the better HER performance the material.

Experimental Section

Preparation of the precursors: 200 mg V_2O_5, 300 mg $Zn(NO_3)_2.6H_2O$, 280 mg hexamethylenetetramine, and 500 mg sodium sulfate were dissolved in 35 mL distilled water under vigorous stirring for 30 min. The obtained mixture was transferred into 50 mL Teflon-lined stainless steel autoclave which was sealed and treated at 110 °C for 24 h in oven. The obtained sample on the bottom of autoclave was ZnV-LDHs precursor. Similarly, ZnVRu-LDHs was prepared based on the same procedure except for the extra 10 mg $RuCl_3.3H_2O$. Then, all the precursors were washed with deionized water and pure ethanol thoroughly, followed by drying overnight in a vacuum oven at 60 °C.

Fabricating hierarchical porous undoped and Ru-doped $Zn_3V_3O_8$: The precursors were put in the middle of the quartz boat which was put in a horizontal quartz tube furnace. A programmed heating process was adopted in the quartz tube furnace under Ar/H_2 (Ar=40 SCCM; H_2=10 SCCM) atmosphere (Detailedly, 25 ^oC to 500 ^oC with a rate of 5 ^oC min^{-1}, and then from 500 ^oC to 600 ^oC with a rate of 1^oC min^{-1}, finally held at 600 ^oC for 120 min). After dissolving ZnO in 0.1 M NaOH solution, the undoped and Ru-doped $Zn_3V_3O_8$ were collected by centrifugation using deionized water.

Characterizations: Scanning electron microscope (FESEM, JSM-7800F), transmission electron microscopy (TEM, Philips, Tecnai, F30) coupled with energy-dispersive X-ray spectrometry (EDS) analyser and high-angle annular dark-file scanning trans-mission electron microscopy (HAADF-STEM) images were collected on JEOL JEMARM200F microscope incorporated with a spherical aberration correction system for STEM; X-ray photoelectron spectroscopy (XPS, PHI 5000 Versaprobe) and powder X-ray diffraction (XRD, Bruker D8 Advance X-ray

diffractometer with Cu Kα radiation) were adopted to characterize the as-prepared samples.

Electrochemical OER and HER tests: The as-synthesized samples were dispersed into a mixed solution of 10 vol.% Nafion (0.5 wt.%) and 90 vol.% ethanol to form a homogeneous slurry which was evenly painted on carbon fiber paper with a catalyst loading of 2 mg cm^{-2} as a working electrode. Saturated calomel electrode (SCE), and graphite rob worked as the reference and counter electrodes, respectively. The three electrode cell with 1.0 M KOH electrolyte was tested on a CHI 660D electrochemical work station (CH Instruments, Inc., Shanghai). The potential values were changed to E (vs. RHE) from E (vs. SCE) according to the formula: $E_{RHE}=E_{SCE}+0.059pH+E_{SCE}^{0}$; the overpotential (η) for OER was calculated according to the following formula: $\eta\ (V) = E_{RHE} - 1.23\ V$.

Figures

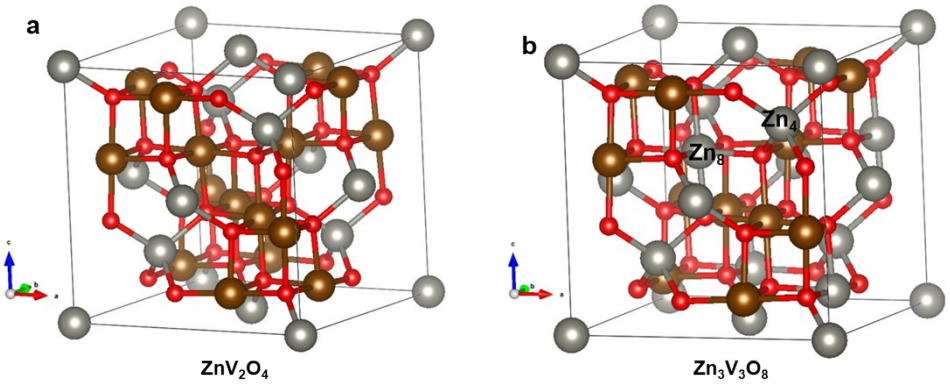

Fig. S1 Structures of ZnV_2O_4 (**a**) and $Zn_3V_3O_8$ (**b**). Brown, grey and red balls represent the V, Zn and O atoms, respectively. Meanwhile, Zn atom at a tetrahedral site and a octahedral site are labeled as Zn_4 and Zn_8, respectively.

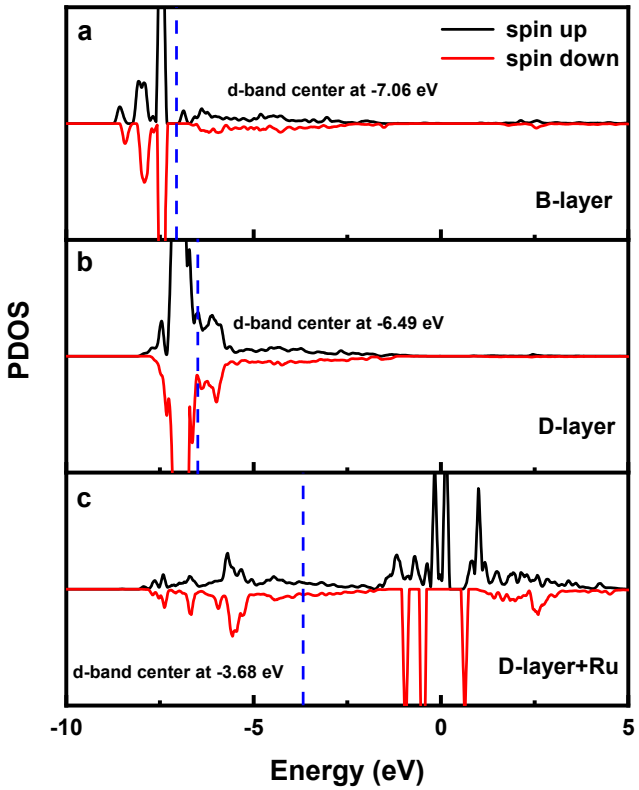

Fig. S2 Projected DOS from d-orbital of Zn_4 at B-layer (**a**), Zn_4 at D-layer (**b**) and Ru at Ru-doped D-layer (**c**).

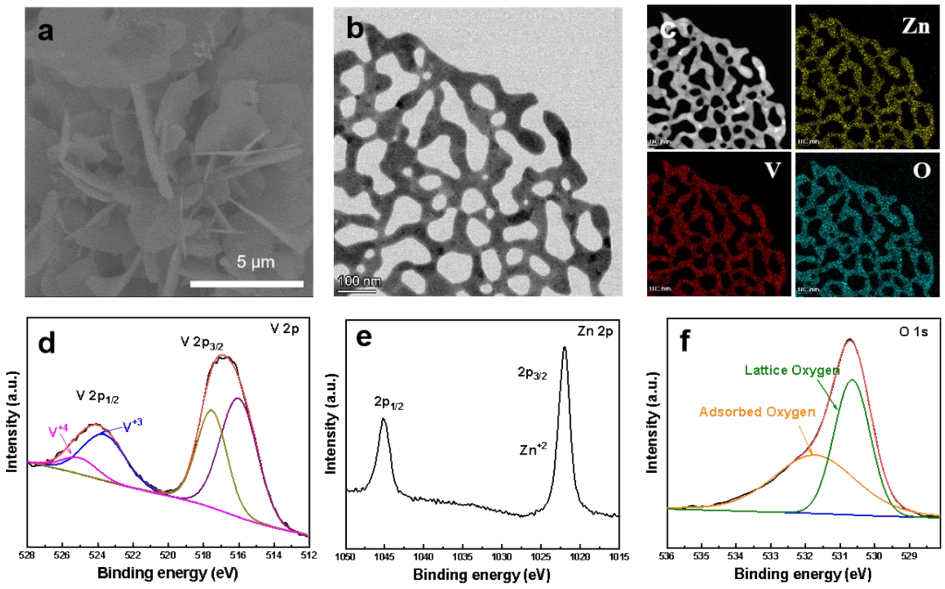

Fig. S3 SEM (**a**) and TEM (**b**) and the corresponding elemental mappings (**c**) of the undoped $Zn_3V_3O_8$ sample. XPS spectra of V 2p (**d**), Zn 2p (**e**) and O 1s (**f**) of the undoped $Zn_3V_3O_8$.

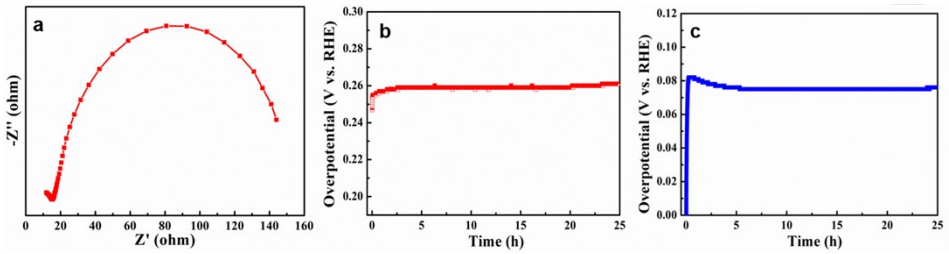

Fig. S4 (**a**) EIS of Ru-doped $Zn_3V_3O_8$ in 1.0 M KOH; (**b**) OER durability test for Ru-doped $Zn_3V_3O_8$ at the current density of 10 mA cm^{-2}; (**c**) HER durability test for Ru-doped $Zn_3V_3O_8$ at the current density of 10 mA cm^{-2}.

Tables

Table S1 Surface energies (E_{surf}) of four terminations. E_{surf} is calculated by the formula: $E_{surf} = \frac{E_{slab} - N \times E_{bulk}}{2A}$, where E_{slab} and E_{bulk} are energies of each termination and $Zn_3V_3O_8$ bulk, respectively.

	A-layer	B-layer	C-layer	D-layer
E_{surf} (eV Å^{-2})	0.103	0.084	0.106	0.086

Table S2 Reaction free energies of each step (U = 0) and overpotentials for the Ru-doped C-layer and D-layer terminations. The rate-limiting steps for each reaction site and the lowest overpotential are highlighted in bold font.

Reaction site		ΔG_1 (eV)	ΔG_2 (eV)	ΔG_3 (eV)	ΔG_4 (eV)	η (V)
C-layer+Ru (replace V)	Ru(V)	-0.12	0.37	**2.66**	2.01	1.43
	V(V)	0.36	0.63	**2.56**	1.37	1.33
C-layer+Ru (replace Zn_8)	Ru(Zn_8)	-0.11	0.51	**2.37**	2.15	**1.14**
	V(Zn_8)	0.30	0.56	**2.65**	1.41	1.42
D-layer+Ru (replace V)	Ru(V)	0.15	0.64	**2.18**	1.95	0.95
	V(V)	0.25	0.73	**2.44**	1.50	1.21
	Zn_4(V)	0.33	**2.48**	0.85	1.26	1.25
D-layer+Ru (replace Zn_4)	Ru(Zn_4)	-0.20	0.41	**2.46**	2.25	1.23
	V(Zn_4)	0.24	0.62	**2.56**	1.50	1.33
	Zn_4(Zn_4)	0.08	**2.51**	0.73	1.60	1.28
D-layer+Ru (replace Zn_8)	Ru(Zn_8)	-0.15	0.93	2.02	**2.12**	**0.89**
	V(Zn_8)	0.38	0.69	**2.09**	1.76	**0.86**
	Zn_4(Zn_8)	-0.02	**2.46**	0.74	1.74	1.23

Table S3 Binding energies (E_{bind}) of Ru on B-layer and D-layer. E_{bind} is calculated by: $E_{\mathrm{bind}} = E_{\mathrm{total}} - E_{\mathrm{sub-Zn/V}} - E_{\mathrm{Ru}}/n$, where E_{total}, $E_{\mathrm{sub-Zn/V}}$ and E_{Ru}/n are energies of Ru doped $Zn_3V_3O_8$, the termination except replacing Zn or V atom and a Ru atom in the bulk, respectively.

	B-layer		D-layer		
	Ru(V)	Ru(Zn_4)	Ru(V)	Ru(Zn_4)	Ru(Zn_8)
E_{bind} (eV)	0.254	3.451	0.580	3.261	0.905

Table S4 Free energies of H adsorption for different reaction sites at the Ru-doped A-layer and B-layer terminations. The small $|\Delta G_{*H}|$ is highlighted in bold font.

Reaction site		ΔG_{*H} (eV)
A-layer+Ru (replace V)	Ru(V)	**0.04**
	V(V)	1.09
B-layer+Ru (replace V)	Ru(V)	0.50
	V(V)	1.41
	Zn_4(V)	0.47
B-layer+Ru (replace Zn_4)	Ru(Zn_4)	-0.60
	V(Zn_4)	1.45
	Zn_4(Zn_4)	**0.27**
C-layer+Ru (replace V)	Ru(V)	**-0.19**
	V(V)	1.00
	Zn_8(V)	1.34
C-layer+Ru (replace Zn_8)	Ru(Zn_8)	**-0.23**
	V(Zn_8)	0.70
	Zn_8(Zn_8)	1.04

Table S5 Zero-point energy (ZPE) and entropy correction (TS) at T = 298 K for relevant species.

Species	ZPE (eV)	TS (eV)
H_2O	0.56	0.67
H_2	0.27	0.41
*OOH	0.35	0
*OH	0.31	0.01
*O	0.05	0
*H	0.19	0

Table S6 Comparison of OER catalytic performances.

Catalyst	Tafel slope (mV/dec)	Overpotential at 10 mA cm^{-2} (mV)	Reference
$Ru/Zn_3V_3O_8$	81.9	250	This work
$NiCo_2O_4$	90	460	*J. Mater. Chem. A,* 2014, **2**, 20823-20831
$Au/NiCo_2O_4$	63	360	*ChemCatChem,* 2014, **6**, 2501-2506
$IrNiO_X$	/	320	*Angew. Chem. Int. Ed.,* 2015, **54**, 2975-2979.
NiC/C	46	316	*Adv. Mater.,* 2016, **28**, 3326
$Zn_xCo_{3-x}O_X$	51	320	*Chem. Mater.,* 2014, **26**, 1889-1895
NiCoP/C	96	330	*Angew. Chem. Int. Ed.,* 2017, **129**, 3955-3958
Ni@graphene	66	370	*ACS Sustainable Chem. Eng.,* 2017, **5**, 4771−4777
VOOH	68	270	*Angew. Chem. Int. Ed.,* 2017, **56**, 573-577
NiV LDH	50	318	*Nat. Commun.,* 2016, **7**, 1-9

Table S7 Comparison of HER catalytic performances.

Catalyst	Tafel slope (mV/dec)	Overpotential at 10 mA cm^{-2} (mV)	Reference
$Ru/Zn_3V_3O_8$	50.6	70	This work
$NiCo_2O_4$	49.7	90	*Angew. Chem. Int. Ed.,* 2016, **55**, 6290-6294
NiP_2 NS/CC	51	75	*Nanoscale,* 2014, **6**, 13440-13445
MoC_x	59	115	*Nat. Commun.,* 2015, **6**, 6512
VOOH	104	164	*Angew. Chem. Int. Ed.,* 2017, **56**, 573-577
NiFe LDH	/	210	*Science,* 2014, **345**, 1593-1596
CoNi@NC	104	224	*Angew. Chem. Int. Ed.,* 2015, **54**, 2100-2104
Pt-CoS_2/CC	82	24	*Adv. Energy Mater.,* 2018, **8**, 1800935
MoC_x@C-1	56	79	*J. Mater. Chem. A,* 2016, **4**, 3947-3954
Ni@graphene	120	240	*ACS Sustainable Chem. Eng.,* 2017, **5**, 4771−4777

References

1 G. Kresse and J. Furthmiiller, *Comp. Mater. Sci.,* 1996, **6,** 15-50.

2 G. Kresse and J. Furthmiiller, *Phys. Rev. B,* 1996, **54,** 11169-11186.

3 G. Kresse and D. Joubert, *Phys. Rev. B,* 1999, **59,** 1758-1775.

4 J. P. Perdew, K. Burke and M. Ernzerhof, *Phys. Rev. Lett.* 1996, **77,** 3965-3868.

5 S. L. Dudarev, G. A. Botton, S. Y. Savrasov, C. J. Humphreys and A. P. Sutton, *Phys. Rev. B,* 1998, **57,** 1505-1509.

6 V. Pardo, S. Blanco-Canosa, F. Rivadulla, D. I. Khomskii, D. Baldomir, H. Wu, and J. Rivas, *Phys. Rev. L*, 2008, **101**, 256403.

7 M. Chase Jr, NIST JANAF Thermochemical Tables; American Institute of Physics: New York, 1998.

8 V. Wang, N. Xu, J.C. Liu, G. Tang, et al, VASPKIT: A Pre- and Post-Processing Program for VASP Code, arXiv:1908.08269.